

Unveiling the acoustics of the Cathedral of Santiago de Compostela using 3D impulse responses

Francesco MARTELLOTTA¹; Angel ALVAREZ CORBACHO²; Lidia ALVAREZ-MORALES³,
Francesca BALESTRA¹, Federica CIANI¹, Miguel GALINDO DEL POZO², Juan José GÓMEZ
ALFAGEME⁴, Pedro Fernando NOGUEIRA LOPEZ⁵

¹ DICAR – Politecnico di Bari, via Orabona 4, Bari, Italy

² IUACC - Universidad de Sevilla, Av. Reina Mercedes 2, 41012 - Sevilla, España

³ Department of Theatre, Film and Television, University of York, York, UK

⁴ ETSIST, Universidad Politécnica de Madrid; Nikola Tesla s/n 28031 Madrid; España

⁵ Dep. de Física y Ciencias de la Tierra, Universidade da Coruña, Rúa da Fraga, 27, 15008 A Coruña; España

ABSTRACT

The Cathedral of Santiago de Compostela in Spain is the arrival point of hundreds of thousands of pilgrims that every year get to the city along the many paths of the “Camino de Santiago”. Along with the oldest part of the city, the cathedral is listed as UNESCO World Heritage, and several restoration works have been done and still are under way. Its acoustics is the result of centuries of evolution since the original Romanesque building was started, with contributions from nearly every architectural style. The interior arrangement of the church is significantly different from the majority of Spanish cathedrals, where the choir typically breaks the main nave creating many sub-spaces. Here the plan follows the Latin cross shape that allows the pilgrims to look at the altar from nearly everywhere, allowing source-receiver distances up to 70m. An acoustic survey that involved different laboratories allowed the collection of monaural, binaural, and B-format impulse responses in different source-receiver combinations. In the present paper, the results pertaining to B-format measurements are presented, discussing the spatial distribution of the acoustic parameters as a function of the directional pattern of the reflection and of the energy distribution among the different spaces of the church.

Keywords: Worship acoustics, Santiago cathedral, 3D impulse response

1. INTRODUCTION

The architecture of Christian churches, throughout its twenty centuries of history, has been responding to the needs and activities that developed inside them, becoming the spatial result of the evolution of liturgical practices(1). The first Early-Christian churches were thought as simple meeting spaces, where the liturgy was considered as the center of the celebration. Later on, churches evolved according to the different architectural types, regional characteristics, often responding to purely “representative” needs. Thus, the original connection between space and function was often lost in favour of the splendor of the space “ad maiorem Dei gloriam”.

The role of sound inside such spaces has always been crucial because, even if the Latin language was the official language of the Church, and most of the faithful were unable to even understand a word, there were preachings and readings that were given in current language, and required better intelligibility. Inside the presbytery, where all the chapter of the priests stood, good intelligibility was also requested. In addition, liturgical music and chanting were also part of the liturgy and, for the previously mentioned reasons, they played the major role in the involvement and participation of the faithful to the celebration. And this introduces a further element of complexity which is related to the natural evolution of the musical language from plain chant to polyphony (2).

The number of mutually connected aspects was therefore quite large, and this, combined with a lack of a clear understanding of the acoustic phenomena, resulted in spaces where the listening experience

¹ francesco.martellotta@poliba.it

was far from optimal. This is further emphasized after the Second Vatican Council (1962-65) which gave greater emphasis to the understanding of the whole liturgy (and not just the preaching), by adopting national languages as a standard.

The number of studies dedicated to church and worship acoustics has been increasing in the last 20 years(3), involving research groups from different countries, and investigating several aspects spanning from the modelling of sound field variations inside them, the role of occupancy, the relationship with liturgy and music, the definition of rating schemes for optimal listening conditions. In many cases, given the specific qualities of the spaces (resulting from different shapes and incremental addition of chapels and other sub-volumes, a certain difficulty to generalize results appeared, so that detailed investigations are needed in order to acoustically characterize each church.

The Cathedral of Santiago de Compostela, within the context of Spanish cathedrals(4) represents a significant exception. In fact, its interior arrangement is significantly different from the majority of Spanish cathedrals, where the choir typically breaks the main nave creating many sub-spaces. Here the plan follows the Latin cross shape that allows the pilgrims to look at the altar from nearly everywhere, according to an interior distribution which is more similar to typical Italian cathedrals. The present paper describes the results of a measurement campaign that was carried out in the church, outlining in particular the results obtained by the use of 3D impulse responses.

2. METHODS

2.1 Building description

The Cathedral of Santiago, was originally built as a small Roman mausoleum of the first century, in which the remains of the Apostle Santiago (AD 44) were buried in the year 813. After the discovery of the apostle's relics, a first chapel was built of stone and terracotta. Being too small to accommodate the faithful, in 899 it was replaced by a temple which was later destroyed by the Muslims and rebuilt in 1003, in a pre-Romanesque style, which converted it into a great pilgrimage cathedral. The final aesthetic revolution, arrived in 1860 with the facade of the Obradoiro in Baroque style. Currently it has a volume of around 42,000 m³, a floor area of 2,511 m², an overall surface of about 18,000 m², and a capacity of 620 seated people.

Its interior is finished in materials such as granite (floor, walls and chorus), plaster (all the temple) glass (windows), wood (pews and confessionals) typically characterized by relatively low absorption coefficients, with the exception of wood and glass that are more absorbing in the low frequencies. This somewhat suggests that the expected reverberation time will be long and strongly dependent on the presence of the faithful who, on the other side, are characterized by a high sound absorption.

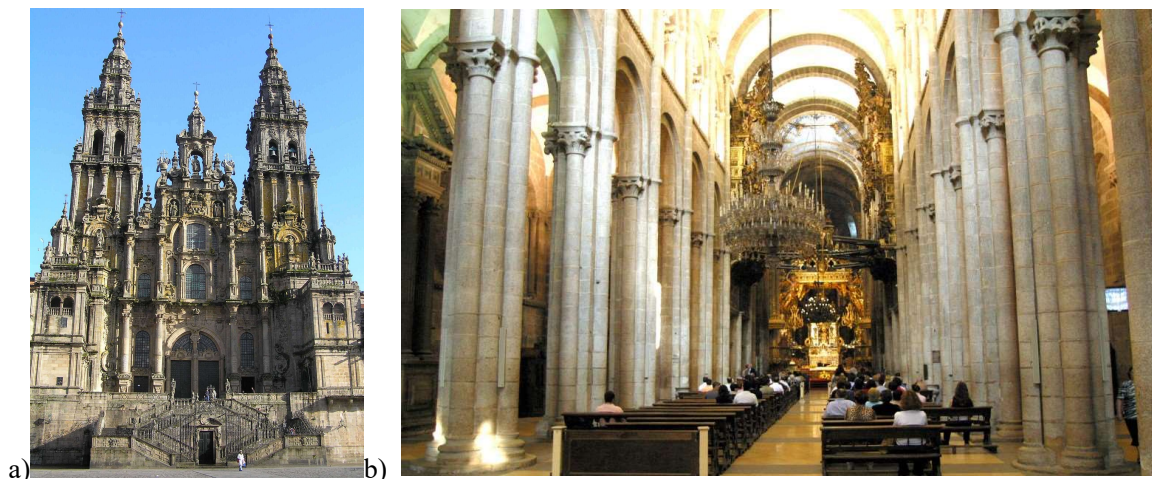


Figure 1 – a) Facade of the Obradoiro, b) interior view of the Cathedral of Santiago de Compostela

2.2 Measurement procedure

The measurements were carried out during the night, in order to minimize background noise, and the requirements of ISO 3382-1 (5), as well as according to the specific prescriptions established for the churches (6,7). With reference to the arrangement of sources and receivers, as the cathedral of Santiago moves away from the typical configuration of the Spanish churches (7), the source was

located at the Main altar (S1), on the pulpit (S2) and at the modern altar (S3). On the pulpit, the source was placed as close as possible to the balustrade to simulate the natural position of the speaker. In all the cases source height was 1.70 m. As the cathedral of Santiago, with Latin cross plan, is almost perfectly symmetrical, the receivers were located in the main nave in only one half of the church, placing only three control receivers in the other half, in the transept braces, and in the presbytery. All the microphones were located at a height of 1.2 from the floor (Figure 2).

The impulse response acquisition process, from which all acoustic parameters were determined (in accordance with ISO 3382-1 (5)), was carried out by different researchers teams, with their own tools, in order to guarantee a complete coverage of the whole church and the detection of all acoustic monaural and binaural parameters. Sound sources included an AVM DO-12 dodecahedron with B&K amplifier 2734, a B&K 4296 source, and a self-built source. The recordings were made using different microphones, including a B-format Soundfield ST350, an Audio-Technica AT4050 / CM5 microphone in its omnidirectional and figure-of-eight configurations, a Head III binaural head (Head Acoustics) connected to a B&K 2829 signal conditioner, and two microphones AKG (omnidirectional and figure-of-eight shaped).

The methodology used by the three research groups was developed with the aim of being the most optimal so that the data could be easily shared and comparable. Impulse responses (IRs) were recorded by exciting the source with a sine sweep spanning from 63 Hz to 16 kHz. The length of the sweep was kept at about 10 s so that the impulse-to-noise ratio (INR) was at least 45 dB at each band for every source receiver combination. Different software tools were used to manage impulse response acquisition. In one case (Bari) the microphone was connected to a four-channel portable recorder (Tascam DR680), and the measurements were carried out in open loop configuration, being subsequently post-processed. The recorded room responses were deconvolved and the resulting IRs were then used to calculate all the acoustical parameters, calculated according to ISO 3382-1(5).

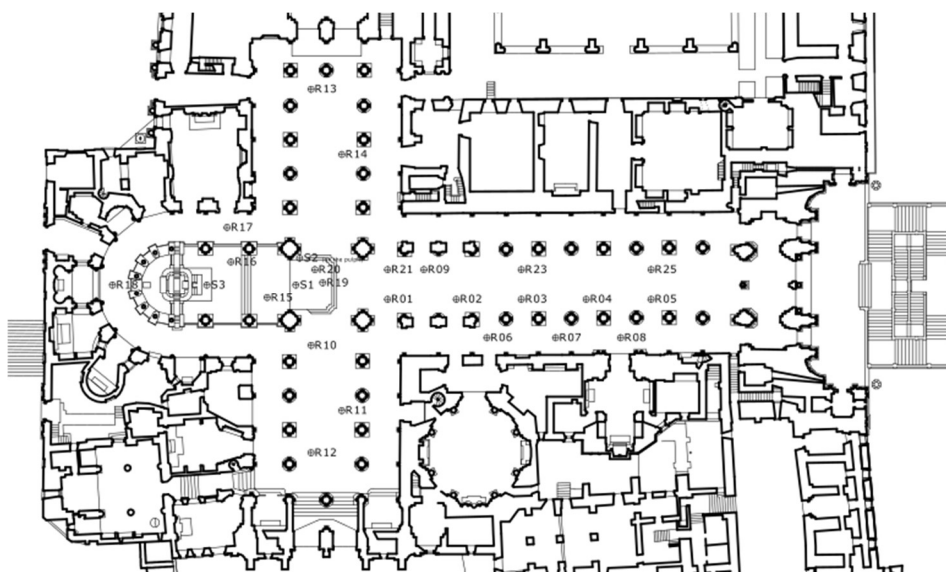


Figure 2 – Plan of the church with source (S) and receiver (R) placement

2.3 3D sound field visualization

Although a thorough description of the procedure to obtain spatial visualization of sound distribution can be found elsewhere(8), it may be useful to quickly remind the basic concepts behind it. Ambisonic microphones provide four signals identified as W, X, Y, and Z. The first one represents the omni-directional response of the microphone at the centre of the microphone array. The others correspond to the 1st order components and provide a figure-of-eight response oriented along each one of the three Cartesian axes. So, they provide the sound pressure multiplied by the vector of the sound direction along that axis. In other words, considering that particle velocity (u) is a vector quantity oriented along the direction of sound propagation, and that (at least for plane waves) u is proportional to sound pressure (p) through characteristic impedance Z_0 ($u=p/Z_0$), X, Y, and Z may also be assumed as the Cartesian components of the particle velocity and used to determine sound intensity properties.

All this stated, considering the relationship between sound intensity, sound pressure and particle velocity, the instantaneous intensity components may be expressed as:

$$\begin{aligned} I_x &= p \cdot u_x = w \cdot x/Z_0 \\ I_y &= p \cdot u_y = w \cdot y/Z_0 \\ I_z &= p \cdot u_z = w \cdot z/Z_0 \end{aligned} \quad (1)$$

Where w , x , y , and z are the output signals of the B-format microphone. At this point, given the I_x , I_y , and I_z components of the sound intensity, the direction of arrival of the sound at a given time may be easily calculated from the following equations:

$$\theta = \text{atan}\left(\frac{I_y}{I_x}\right); \phi = \text{atan}\left(\frac{I_z}{\sqrt{I_x^2 + I_y^2}}\right) \quad (2)$$

So, combining together the direction of sound with its intensity, sound field properties may be reproduced using a multichannel loudspeaker system or, as in the present case, used to obtain a spatial map of the sound intensity as a function of time.

3. RESULTS

3.1 Mean values of acoustical parameters

First of all the spatially averaged values as a function of frequency and source position were analyzed. For reverberation time (T30) no substantial differences appeared as a function of source position (Fig. 3a), while in terms of frequency, substantially stable values appeared up to 500 Hz, then rapidly decreasing as a consequence of air absorption. When early decay time (EDT) was considered (Fig. 3b), the shortest values appeared when source S3 was used, while the longest appeared when the source was on the pulpit. However, a significant scatter in data was observed, with standard deviations as large as 2 s in the frequency bands below 1 kHz and very short values observed close to the source. Center time (Ts) and clarity (C80) both showed similar variations as a function of frequency and source position (Fig. 4), with the lowest clarity values (and the longest Ts values) observed when source was on the pulpit. The explanation of this rather counter-intuitive result stands in the fact that the receivers included in each average differ slightly as a function of source position, so that a larger number of receivers closer to the sound source may lower the mean values, but this does not imply that points at comparable distance behave differently.

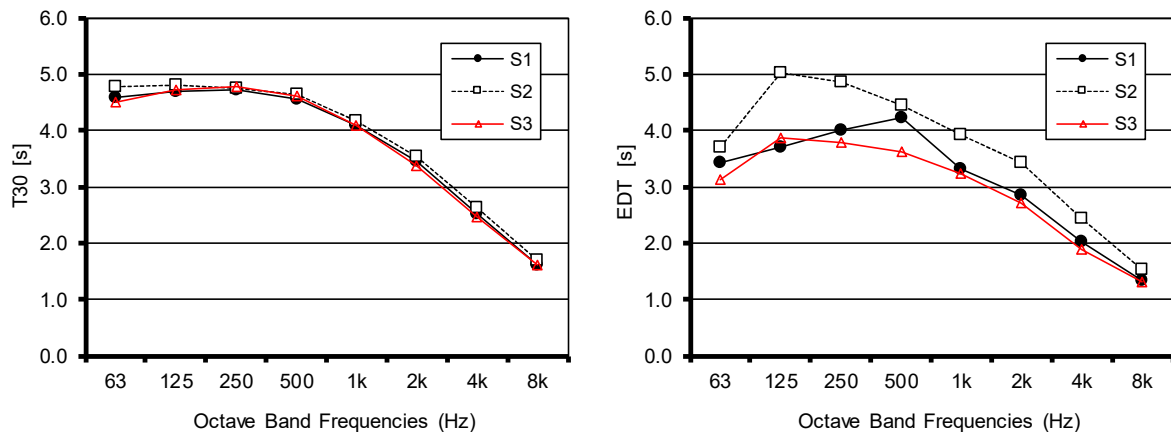


Figure 3 – Plot of spatially averaged T30 (a) and EDT (b) values measured as a function of frequency and of source position

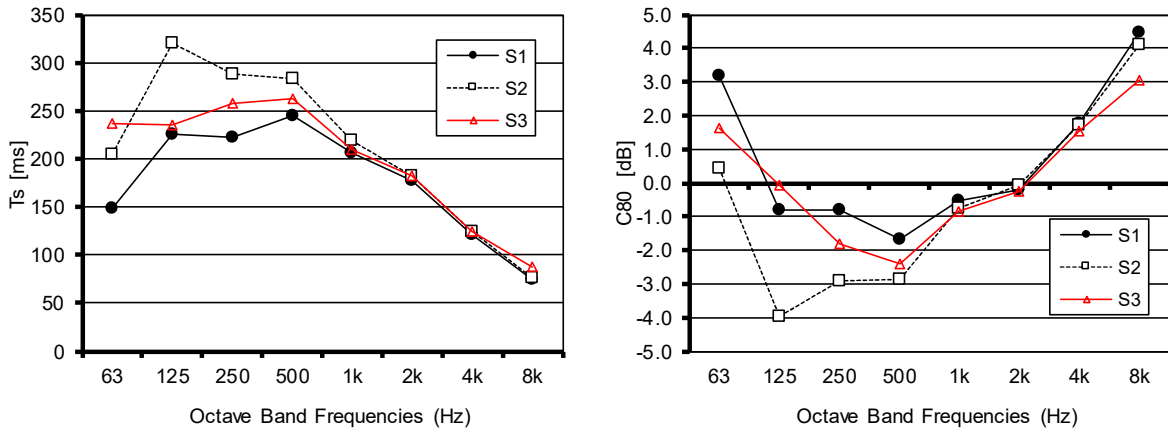


Figure 4 – Plot of spatially averaged T_s (a) and $C80$ (b) values measured as a function of frequency and of source position

3.2 Effect of source receiver distance

In order to better understand some of the behaviors observed before, the parameters were plotted as a function of source receiver distance for selected frequency bands. In case of EDT (Fig. 5a) the plot showed a quite varied condition, with significantly shorter values at receivers close to sound sources. However, distance proved not to be the only influencing factor, as receivers 10 and 16 behaved quite differently when source S1 (which is at nearly the same distance of about 9 m) was used. Receiver 16 had an EDT very close to the spatially averaged T_{30} value, while receiver 16 was shorter than 2 s. The latter was located inside the presbytery area, where double slopes were clearly detected by means of Bayesian analysis (9). In fact, Figure 5b showed that at R16 the first decay process was characterized by a reverberation time of about 1 s, while the second one, appearing after about 0.5 s, clearly had the same value of the mean T_{30} .

The mid-frequency values of T_s and $C80$ were also plotted as a function of source receiver distance (Figure 6). In this case, in order to provide a reference, predicted values obtained by means of the “revised model”(10-12) were also plotted. Values were calculated assuming the geometric parameters given before and assuming the constant terms $s=0.2$ (suitable when the source is raised and surrounded by reflecting surfaces), and $k=2.8$ (corresponding to a space with a richly articulated volume). It is interesting to observe that values pertaining to sources S1 and S2 fitted well with predicted values, showing the typical exponential variation as a function of distance. Conversely, results pertaining to source S3 appeared shifted, with clarity which was 3 dB higher compared to points at the same distance, and T_s which was about 75 ms shorter than points at comparable distance.

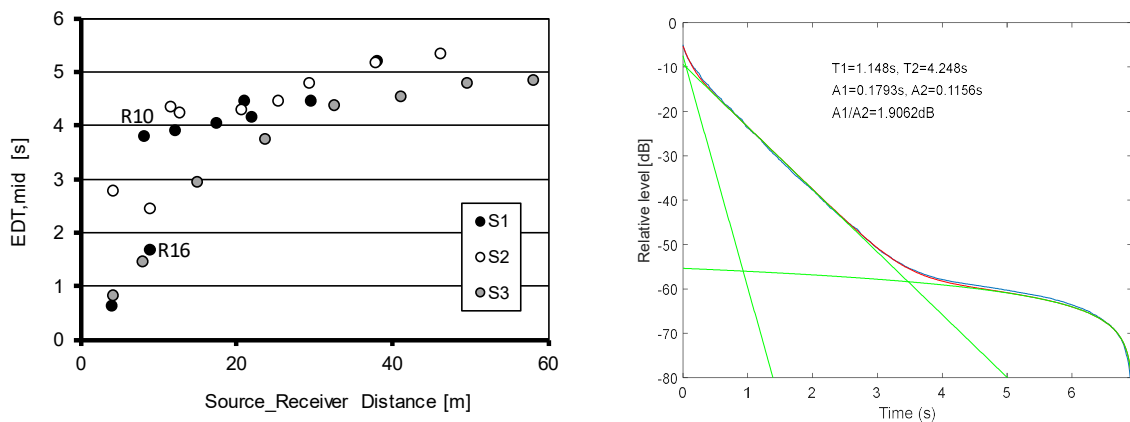


Figure 5 – a) Plot of mid-frequency values EDT as a function of source receiver distance and source position. b) Results of Bayesian analysis applied to S1-R16 at 1 kHz.

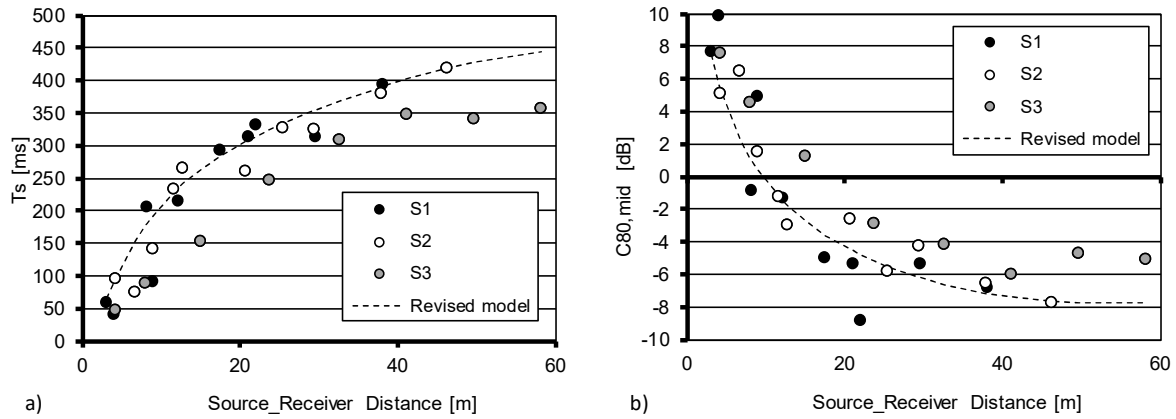


Figure 6 – Plot of mid-frequency values of a) T_s and b) $C_{80, \text{mid}}$ as a function of source receiver distance and source position. Revised model was applied by assigning the characteristic parameters $s=0.2$ and $k=2.8$.

A substantially similar behavior was observed also at other frequencies, with the significant exception of the lowest bands, where, as already observed, source S2 showed markedly lower C_{80} values and higher T_s . Realistically, the position of source S2, although raised, offered little support to lower frequencies which were diffracted by the pillar rather than reflected. Conversely, source S3 which stood in a well isolated sub-volume (and during measurements the presence of scaffolding on the top of the presbytery caused a further reduction of the available space), benefitted of increased early reflections that realistically caused the observed variations. In order to better clarify such aspects 3D mapping offered a significant support.

3.3 3D sound maps

Following the observations made in the previous section it was interesting to compare different source receiver combinations corresponding to similar distances in terms of directional distribution of reflections. As a first example combinations S1-R02 and S3-R01 were considered (Figure 7), corresponding respectively to 21.1 m and 23.8 m. In the second case, even though the distance was bigger, the direct sound was louder, and stronger early reflections, mostly coming from the presbytery area were observed. Conversely, in the first case, reflections arriving in the first 100 ms after direct sound were more diffuse, arriving mostly from the front and the sides, but definitely less loud. Such difference in the direction of arrival was also proved by the different J_{LF} values, which were 0.34 in the first case and 0.19 in the second.

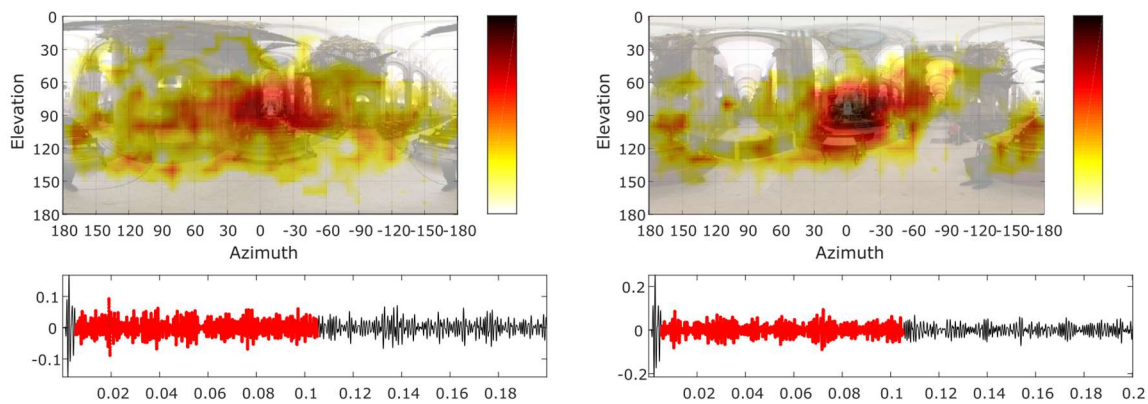


Figure 7 – 3D sound map at 1 kHz octave band of: a) S1-R02; b) S3-R01. In all the cases a 100 ms time interval is considered, starting 5 ms after direct sound

The second pair of IRs that were analyzed were S2-R05 and S3-R04 (Figure 8), with source-receiver distances respectively of 46.3 m and 49.7 m. It was interesting to notice that, in this case, most of the reflections were focused along the longitudinal axis, with a clear dominance of frontal reflections. In particular, when the source was located on the pulpit the lack of large reflecting surfaces (and the significant diffraction and scattering effects) caused amore circumscribed distribution of the reflections around the source-receiver direction. Conversely, when the source was close to the main altar, the direction of arrival of the early reflections spread over an angle of $\pm 30^\circ$ and contributions were generally stronger. This difference in angular distribution of reflections could be found also in J_{LF} values, equal to 0.126 for S02-R05 and to 0.153 for S03-R04.

So, taking into account both the previous results, what emerges clearly is an important role of the main altar and of the surrounding surfaces (it is important to remember that quite unusually, the spans of the presbytery are closed with thick glass surfaces, that ensure further strong reflections coming from that area), in increasing the number and magnitude of early reflections. When the source is at the modern altar or on the pulpit the reflections appeared weaker and scattered.

In order to better clarify the role of the surfaces around the presbytery, combination S3-R16 was finally analyzed, taking into account different time intervals. As shown in Figure 9, the early reflections clearly arrive from the closest and hardest surfaces (like the floor and the glazed elements that close the bays), and they continue arriving from within the same subspace up to about 0.5 s. After that time, diffuse sound reflections coming from the main church volume start arriving and they contribute more and more to the late sound decay.

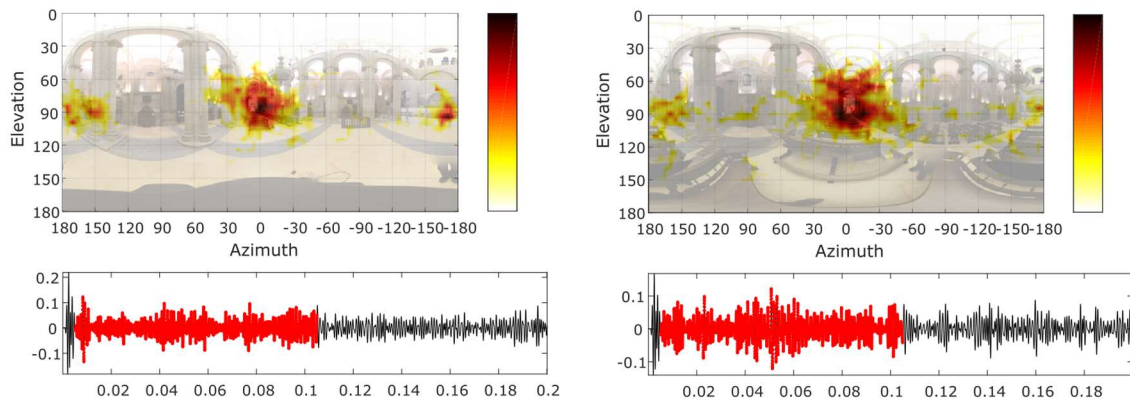


Figure 8 – 3D sound map at 1 kHz octave band of: a) S2-R05; b) S3-R04. In all the cases a 100 ms time interval is considered, starting 5 ms after direct sound

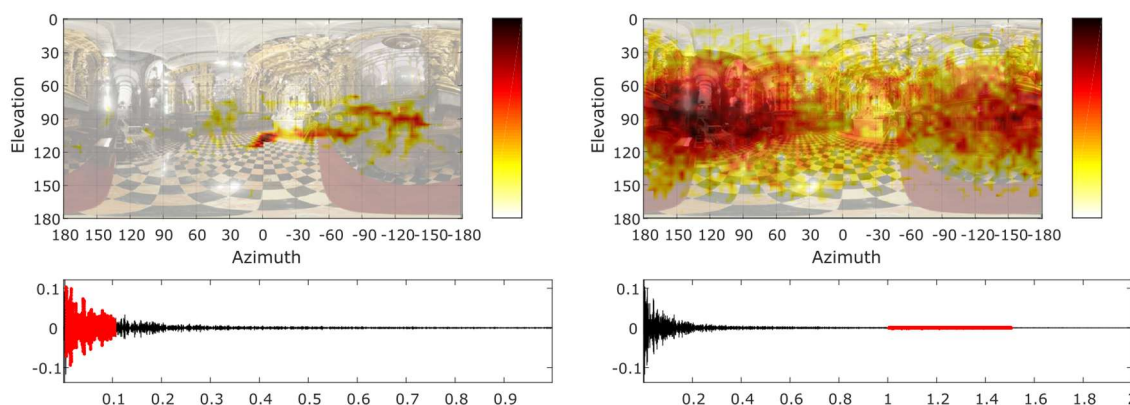


Figure 9 – 3D sound map at 1 kHz octave band of S3-R16: a) considering a 100 ms time interval, starting 5 ms after direct sound; b) considering a 0.5 s starting from 1 s after direct sound arrival

4. CONCLUSIONS

The results of the measurements carried out in the Cathedral of Santiago de Compostela have been presented in the paper. The church represents a significant exception among the Spanish cathedrals because of the lack of the choir opposite to the presbytery that typically closes the central nave. This solution, adopted for the benefit of the many pilgrims that attend the celebrations, makes the church more similar to Italian models. The analysis of the acoustical parameters pointed out significant variations as a function of source and receiver placement. In particular, presbytery area which is characterized by a significant amount of reflecting surfaces (bays are closed by glazings and a scaffolding reduced the available height at the time of the measurements) affected significantly both source and receivers located inside it. With reference to the source, the 3D sound maps confirmed that extra reflections provided by the surfaces contributed to increase magnitude and number of early reflections, so that a 3 dB improvement in clarity (and a decrease of 75 ms in center time) values was found as a function of distance. Comparison with predictive models, also showed that values pertaining to other sources were in good agreement with the expected behavior, while the source at the high altar provided quite unusual results. With reference to receivers inside the presbytery, they showed double slopes, independent of the source position (but clearly emphasized when the source was inside the same space). Again 3D sound maps clearly showed that up to about 0.5 s reflections arrived mostly from surfaces inside the presbytery, while after that time the dominant contribution arrives from diffuse reflections from the main nave. A more detailed analysis is under way to better clarify the role of source and receiver placement with reference to other combinations (e.g. located in the transept), as well as in order to provide a more thorough analysis including the results of all the teams participating to the project.

ACKNOWLEDGEMENTS

Authors are grateful to the Santiago Cathedral Foundation for giving us access to the acoustic and archival study of this magnificent place, and to Jose Carlos Alonso Seoane, parish priest of the Church of Santa Cruz de Oleiros (A Coruña) for his contribution to the organization of the measurements.

REFERENCES

1. Suarez R, Sendra JJ, Alonso A. Acoustics, Liturgy and Architecture in the Early Christian Church. From the domus ecclesiae to the basilica. *Acta Acustica united with Acustica*. 2013; 99(2): 292-301.
2. Cirillo E, Martellotta F, Worship, acoustics, and architecture. Multi-science publishing, Brentwood; 2006.
3. Girón S, Álvarez-Morales L, Zamarreño T. Church acoustics: A state-of-the-art review after several decades of research. *J. Sound Vib.* 2019; 411: 378-408.
4. Álvarez-Morales L, Girón S, Galindo M, Zamarreño T. Acoustic Environment of Andalusian Cathedrals. *Build. Environ.* 2016; 103: 182-192.
5. ISO 3382-1:2009. Acoustics-Measurement of room acoustic parameters, Part 1: Performance spaces, International Organization for Standardization, Geneva, Switzerland; 2009.
6. Martellotta F, Cirillo E, Carbonari A, Ricciardi P. Guidelines for acoustical measurements in churches. *Appl. Acoust.* 2009; 70: 378-388.
7. Álvarez-Morales L, Zamarreño T, Girón S, Galindo M. A methodology for the study of the acoustic environment of Catholic cathedrals: application to the Cathedral of Malaga. *Build. Environ.* 2014; 72: 102-115.
8. Martellotta F. On the use of microphone arrays to visualize spatial sound field information. *Appl. Acoust.* 2013; 74: 987-1000.
9. Xiang N, Goggans P, Jasa T, Robinson P. Bayesian characterization of multiple-slope sound energy decays in coupled-volume systems. *J. Acoust. Soc. Am.* 2011; 129: 741-752.
10. Martellotta F, A multi-rate decay model to predict energy-based acoustic parameters in churches. *J. Acoust. Soc. Am.* 2009; 125(3): 1281-1284.
11. Berardi U, Cirillo E, Martellotta F., A comparative analysis of acoustic energy models for churches. *J. Acoust. Soc. Am.* 2009; 126(4): 1838-1849.
12. D'Orazio, D., Fratoni, G., Garai, M., Acoustics of a chamber music hall inside a former church by means of sound energy distribution. *Canadian Acoustics*. 2017; 45(4): 7-17